

Cardiac Flow Analysis Using Magnetic Resonance Imaging

by

Kelvin K. L. Wong

B.Eng (Hons), Nanyang Technological University, 2001
Master Appl. I.T., The University of Sydney, 2003

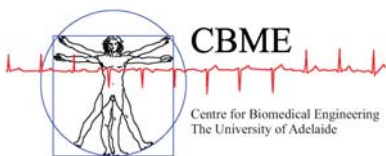
Thesis submitted for the degree of

Doctor of Philosophy

in

School of Electrical and Electronic Engineering,
Faculty of Engineering, Computer and Mathematical Sciences
The University of Adelaide

August, 2009



© 2009
Kelvin K. L. Wong
All Rights Reserved



Contents

Contents	iii
Abstract	xi
Statement of Originality	xiii
Acknowledgments	xv
Conventions	xix
Awards	xxi
Publications	xxiii
List of Symbols	xxv
Abbreviations	xxix
List of Figures	xxxii
List of Tables	xxxvii
Chapter 1. Introduction	1
1.1 Motivation for Flow Imaging in Cardiac Assessment	2
1.2 Review of Current Technologies	5
1.2.1 Velocity-Encoded Magnetic Resonance Imaging	5
1.2.2 Colour Doppler Sonography	7
1.2.3 Other Cardiovascular Flow Measurement Techniques	8
1.3 Cardiac Flow Visualisation Based on Computer Simulation	8
1.4 Applications and Motivation of This Study	11
1.4.1 Assessment of Myocardial Abnormalities	11
1.4.2 Assessment of Bio-Prosthetic Heart Valve Implants	11

1.4.3	Examination of Cardiac Functionalities	12
1.4.4	Assessment of Cardiac Behaviour during Heart Exercise	12
1.5	Outline of Approach	13
1.6	Overview of Research Strategy and Implementation	16
1.7	Statement of Original Contributions	19
1.7.1	Original Contributions to Medical Imaging	19
1.7.2	Contribution to Medical Science and Knowledge	20
Chapter 2. Theory of Magnetic Resonance Imaging		23
2.1	Introduction	24
2.2	Theory of Nuclear Magnetic Resonance Imaging	24
2.2.1	Quantum Mechanics of Magnetic Resonance	24
2.2.2	Magnetic Resonance Imaging Protocols	28
2.3	Asynchronous Precession of Proton in Turbulent Flow	30
2.4	Application of MRI onto Cardiac Diagnosis	31
2.5	Phase Contrast MRI Velocimetry	35
2.5.1	Theory of Phase Contrast MRI	36
2.5.2	Phase Contrast MR Imaging of Cardiac Chambers	36
2.6	Chapter Summary	38
Chapter 3. Implementation of Magnetic Resonance Fluid Motion Tracking		41
3.1	Introduction	42
3.2	Overview of Optical Flow	42
3.3	Lucas Kanade Optical Flow	44
3.4	Multi-Resolution Motion Estimation	46
3.4.1	Definition of Problem	46
3.4.2	Feature Tracking Using Pyramidal Optical Flow	47
3.5	Pyramidal Lucas Kanade Optical Flow	49
3.5.1	Initial Definition	49
3.5.2	Pyramidal Representation of Images	49
3.5.3	Pyramidal Feature Tracking	51

3.5.4	Iterative Lucas Kanade Optical Flow	52
3.6	Filtration of Flow Vector Outliers	55
3.7	MR Fluid Motion Estimation Framework	56
3.7.1	Flow Estimation Using Magnetic Resonance Images	56
3.7.2	Non-Stationary Patterns of Varying Intensity in Cine-MRI	57
3.7.3	Motion Estimation of MR-Signals	57
3.7.4	Effect of Scan Resolution and Image Quality	58
3.7.5	MR Fluid Velocity Field	59
3.8	MR Fluid Motion Tracking System Implementation	61
3.9	Discussion	63
3.10	Chapter Summary	64
 Chapter 4. Computational Validation of Fluid Motion Tracking		65
4.1	Introduction	66
4.2	Data Generation	66
4.2.1	Analytical Formulation of Vortex	66
4.2.2	Generating Vortex Tracks for Artificial Data	67
4.2.3	Variation of Vortical Track Interval Size	69
4.2.4	Configuration of Tracking Features	69
4.2.5	Variation of Image and Optical Flow Window Size	70
4.2.6	Variation of Noise Addition and Smoothing Filter Mask Size	70
4.3	Computational and Analytical Data Differencing	71
4.3.1	Fluid Motion Estimation Flow Predictions	71
4.3.2	Magnitude of Velocity Vectors in Radial Direction	71
4.3.3	Magnitude of Velocity Vectors in Image Representation	72
4.3.4	Direction of Velocity Vectors in Image Representation	72
4.4	Computational Versus Analytical Results	73
4.4.1	Velocity in Image Representation	73
4.4.2	Velocity in Radial Direction	75
4.5	Limitations of Study	84
4.6	Chapter Summary	85

Chapter 5. Visualisation Methods for Cardiac Flow	87
5.1 Introduction	88
5.2 Segmentation of Intra-Cardiac Flow Region	89
5.2.1 Introduction to Active Contour Technique	89
5.2.2 Energy Minimisation of Parametric Snake	89
5.2.3 Implementation of Parametric Snake Model	90
5.2.4 Segmentation of Cardiac Chamber Using Active Contouring	91
5.3 Two-Dimensional Flow Image Reconstruction	93
5.4 Three-Dimensional Flow Image Reconstruction	96
5.4.1 Cartesian Grid for Image and Flow Display	96
5.4.2 Computation of Flow Grid	99
5.5 System Limitations	102
5.6 Chapter Summary	103
Chapter 6. System Design for Visualisation of Vorticity	105
6.1 Introduction	106
6.2 Methods for Visualisation of Vortices	107
6.3 Differential Quantities of Flow	108
6.3.1 First Order Finite Differentiation	108
6.3.2 Vorticity	111
6.3.3 Shear Strain Rate	112
6.3.4 Normal Strain Rate	113
6.4 Statistics of Differential Flow Map	114
6.5 Vortex Visualisation Using Theoretical Formulation	117
6.5.1 Formulation of Vortex Flow Field	117
6.5.2 Variation of Flow Field Resolution	118
6.5.3 Configuration for Vorticity Measurement	119
6.6 Discussion	136
6.6.1 Reliability of Vorticity Measurement	136
6.6.2 Comparison of Vorticity Measurement	137
6.6.3 Effect of Grid Resolution on Vorticity Measurement	142
6.6.4 Limitations of Study	144
6.7 Chapter Summary	145

Chapter 7. Methods of Cardiac Flow Analysis	147
7.1 Introduction	148
7.1.1 Importance of Cardiac Flow Analysis	148
7.1.2 Details of Methods and Analysis in General	149
7.2 Vorticity Visualisation System Implementation	150
7.2.1 Visual Tools for Presentation of Flow Fields	151
7.2.2 System Integration	151
7.3 Experiments	154
7.3.1 Case Study and MRI Scan Procedure	154
7.3.2 Flow Grid Representation	157
7.3.3 Parameters for Data Analysis	160
7.4 Flow Analysis Based on Phase Contrast MR Imaging	161
7.4.1 Flow in the Right Atrium	161
7.4.2 Circulation of Blood in the Right Atrium and Ventricle	164
7.4.3 Analysis of Vorticity in Left Atrial Flow	165
7.5 Introduction to Cardiac Flow Component Analysis	176
7.5.1 Colour-Based <i>K</i> -Means Clustering Segmentation	176
7.5.2 Segregation of Vortices	177
7.5.3 Component Flow Analysis Results	178
7.5.4 Statistics of Component Flow	180
7.5.5 Mechanics of Flow with Reference to the Cardiac Events	181
7.5.6 Limitations of Study	182
7.6 Validating Intra-cardiac Flow Tracking Using Velocity-encoded Imaging	190
7.6.1 Imaging and Flow Visualisation Parameters	190
7.6.2 Implementation of Vorticity Field Differencing	192
7.6.3 Experimental Parameters for Flow Comparison	194
7.6.4 Comparison of Flow-Imaging Results	194
7.6.5 Discussion of System Performance	199
7.7 Chapter Summary	200
Chapter 8. Study of Cardiac Flow in a Heart with Atrial Septal Defect	203

8.1	Introduction	204
8.2	Overview of Atrial Septal Defect	204
8.3	Current Methods in Diagnosing Atrial Septal Defect	208
8.3.1	Echocardiogram	208
8.3.2	Cardiac Magnetic Resonance Imaging	209
8.3.3	Chest Radiography	210
8.3.4	Computed Tomography	210
8.4	Methodology	211
8.4.1	Subject for Case Study	211
8.4.2	MRI Scan Procedure	212
8.4.3	Clinical Investigation	212
8.4.4	Parameters for Data Analysis	212
8.4.5	Investigation Procedure	213
8.4.6	Flow Visualisation System Implementation	216
8.5	Results and Discussion	217
8.6	Flow Analysis	228
8.6.1	Qualitative Flow Analysis	228
8.6.2	Quantitative Flow Analysis	229
8.6.3	Statistical Comparison of Vorticity Maps	230
8.7	Summary of Cardiac Investigation	233
8.8	Discussion of Investigation	234
8.9	Chapter Summary	235
Chapter 9. Conclusion		237
9.1	Introduction	238
9.2	Thesis Summary	238
9.3	Research Novelty	240
9.3.1	Motion Estimation of Degradable Non-Rigid Objects	241
9.3.2	Measures from Cardiac Flow Field	242
9.3.3	Three-Dimensional Grid Reconstruction Using Images	242
9.4	Generation of Interest to Scientific Community	243

9.4.1 Clinical Relevance	243
9.5 Future Directions	244
9.6 Summary of Original Contributions	246
9.7 In Closing	248
Appendix A. Software Implementation of Medflován	251
A.1 Imaging and Visualisation Computing Libraries	252
A.1.1 OpenGL	252
A.1.2 OpenCV	252
A.2 DICOM Decoder Library	255
A.3 The Medflován Software Architecture	255
A.3.1 Package Diagram	256
A.3.2 Use Case Diagram	258
A.3.3 Component Class Diagrams	268
Appendix B. Procedures for MRI Preparation and Processing	283
B.1 MRI Equipment	284
B.2 Imaging and Analysis Procedures	284
Appendix C. Flow Visualisation of Blood in Normal Atrium	289
Appendix D. Visualisation of Right Atrial Flow (Pre-Atrial Septal Occulsion)	309
Appendix E. Visualisation of Right Atrial Flow (Post-Atrial Septal Occulsion)	313
Appendix F. Supplementary Video Clips	317
Appendix G. Particle Image Velocimetry Based on Fluid Motion Estimation	323
G.1 Fluid Motion Estimation Using Particle Images	324
G.1.1 Particle Image Velocimetry	324
G.1.2 Cross-Correlation Versus Pyramidal Optical Flow	324
G.2 Results Generated by Particle Image Velocimetry	326
G.3 Results Generated by Optical Flow	327

Contents

Bibliography	331
Index	355
Résumé	359
Scientific Genealogy	361

Abstract

Many types of cardiac abnormality have an implication on blood flow. However, most present-day diagnostic modalities analyse myocardial structures and not the cardiac flow within to detect heart defects *in vivo*. Currently, various imaging modalities, such as echocardiography, single photon emission computed tomography (SPECT), positron emission tomography (PET), X-ray computed tomography (CT), and cardiac magnetic resonance imaging (CMRI) provide a non-invasive approach for scanning humans with heart abnormalities, and are utilised in the management of cardiac patients. There is a need to develop a visualisation system for analysing flow of blood within the human heart. Motional properties of blood can be measured against normal controls and patients with cardiac abnormalities in order to discover underlying cause of these flow phenomena. This can potentially extend medical knowledge of the defects and their hemodynamic behaviour.

We characterise motion patterns of blood in the human heart and analyse the flow properties, by means of tracking, using a series of time dependent magnetic resonance images. An indication of flow vortices can be provided by numerical computation of vorticity values within the defined region of blood flow. The global estimation of parametric motion flow fields over the whole image provides useful information on the presence of vortices within the heart chamber that can be used to assess cardiac functions. In this study, the crucial strategies for this approach are implemented, and the achievable diagnostic results and quality of assessment are investigated. The developmental stages of the framework and system design of each component for cardiac diagnosis are detailed in this thesis. The key objectives of the research and development for this diagnostic system are implemented herein:

1. Realisation of a non-invasive technique to compute flow features within cardiac structures. System evaluation and velocity calibration of the flow tracker are incorporated in the study. Verification of calculated flow in time-resolved cardiac vessels is performed by error analysis using flow fields constructed by velocity-encoded magnetic resonance imaging velocimetry.
2. Measurement of cardiac vorticities in heart chambers is performed for investigation of flow phenomena. We examine the time-dependent behaviour of cardiac

flow structures in the heart. The variation of flow patterns that are associated with myocardial wall deformations and pressure changes is analysed.

3. Realisation of a statistical framework for examining variations of flow due to myocardial defects in the heart. The quantification of flow will offer the potential to complement diagnostic methods that analyse cardiac defects and evaluate patient condition after surgical intervention.

As an alternative to established medical imaging-based diagnostic techniques such as chest X-rays, and pulsed or continuous wave Doppler ultrasound scans for cardiac diagnosis, we develop a magnetic resonance imaging based approach and perform flow quantification to analyse the heart, *vis-à-vis* blood movement in chambers based on a measured flow field. This framework offers potential for non-invasive flow visualisation in cardiac structures. We validate this methodology specifically for analysing flow characteristics within a human heart case study. We also demonstrate the potential for non-invasive assessment of cardiac abnormality for a pathological case of the heart.

Statement of Originality

This work contains no material that has been accepted for the award of any other degree or diploma in any university or other tertiary institution and, to the best of my knowledge and belief, contains no material previously published or written by another person, except where due reference has been made in the text.

I give consent to this copy of the thesis, when deposited in the University Library, being available for loan, photocopying, and dissemination through the library digital thesis collection, subject to the provisions of the Copyright Act 1968.

I also give permission for the digital version of my thesis to be made available on the web, via the University's digital research repository, the Library catalogue, the Australasian Digital Thesis Program (ADTP) and also through web search engines, unless permission has been granted by the University to restrict access for a period of time.

Signed

Date

Acknowledgments

My supervisors during the course of the PhD study are Professors Jagannath Mazumdar, Derek Abbott, Richard Malcolm Kelso, Stephen Grant Worthley, and Prasthanthan Sanders. Apart from them, a great number of people have collaborated to make this thesis possible. Their support, encouragement, and exchange of ideas have been mind enriching and paved the way for a fruitful research during my study at the University of Adelaide.

Supervision and Mentorship

I would like to convey my warmest appreciation to **Prof Jagannath Mazumdar** for encouraging me to broaden my range of knowledge in medical imaging, biomechanics, and flow visualisation. His advice has motivated me to effectively integrate them into a successful research thesis that I present here. He has also assisted me in establishing important working relationships with medical experts and paved the ways for research collaboration with professional bodies. For his practical contribution, moral support and ever lasting friendship, I owe him a great depth of gratitude.

I am deeply indebted to **Prof Derek Abbott** for his support in my mental and career development. He has imparted to me his invaluable experience and knowledge that has allowed me to develop a unique philosophy of excelling in research. Apart from his patient guidance throughout these years, he has also strengthened my motivation to be knowledgeable in the field of computer tomography and medical image visualisation. Therefore, I also acknowledge him to be an important person to have influenced and groomed my research career.

Special appreciation is extended to **Assoc Prof Richard M. Kelso** from the School of Mechanical Engineering for imparting his knowledge in fluid mechanics, as well as image velocimetry, which are utilised in the development of the techniques used in this study. I sincerely thank his generous contribution of time in my education. He has taught me the important concepts used in flow visualisation methods and groomed me to be a confident and motivated researcher. I look up to him as the best teacher in fluid mechanics.

Acknowledgments

I have the pleasure of working in the Cardiovascular Research Centre (CRC) and Faculty of Health Science that is based at the Royal Adelaide Hospital and the University of Adelaide. **Prof Prashanthan Sanders** and **Prof Stephen G. Worthley** in the School of Medicine have supervised and supported me in the technical and instrumental portions of this thesis, particularly in magnetic resonance imaging. I thank them sincerely for providing me with a fertile environment to crystallise ideas and transforming them into successful outcomes.

Financial Support

I gratefully acknowledge that my scholarship was personally funded by **Prof Derek Abbott** and partly by the Cardiovascular Research Centre (CRC). In addition, the funding for the purchase of software, textbooks and equipment during the course of my work was provided by **Prof Derek Abbott** and **Prof Stephen G. Worthley**. Travel funding to conferences was contributed by Prof Abbott and the School of Electrical & Electronic Engineering.

Commercialisation

I also convey appreciation to **Dr Matthew Chong** from the Adelaide Research and Innovation Pty Ltd for his useful advice in relation to technology transfer and intellectual property rights. He has assisted me in commercialisation of the software deliverable from my research.

Proof Reading and Discussion

It is also a great pleasure to express my gratitude to **Professor Derek Abbott** and **Dr Peter Cooke** at the School of Electrical & Electronic Engineering, as well as **Assoc Prof Richard M. Kelso** for proof reading this thesis. Their advice in scientific writing and referencing has been tremendously helpful.

I thank **Dr Pawel Kuklik** at the Faculty of Health Science and School of Medicine for his encouragement and interest in this work. He has streamlined the discussion of important concepts used in my research. I am delighted to acknowledge **Dr Mathias Baumert** for checking the technical accuracy of my publications and this thesis.

MRI Scanning and Data

The assistance during the scanning of test subjects that is rendered by **Dr Payman Molaee** and **Mr Angelo Carbone** at the Faculty of Health Science and School of Medicine has been invaluable. The supply of magnetic resonance images by the Royal Adelaide Hospital is appreciated. I also thank them for imparting to me their knowledge of medical imaging.

Software Development and Programming

Appreciation is extended to my colleague **Mr Shaoming Zhu** for his assistance in programming the statistical library package of the medical image processing software that is used in my work, and also to **Ms Yumay Chen** for her input in data preparation during program testing. Thanks are also due to **Mr Ishwor Gurung** for his patient help in debugging during the development of graphical user interface for the subsequent version of the software. The advice given by my colleagues **Mr Withawat Withayachumnankul**, **Ms Shaghik Atakaramians** and **Ms Gretel Png**, during the typesetting of my thesis in Latex, is gratefully acknowledged.

Emotional and Mental Support

Special appreciation goes out to the rest of my colleagues in the Centre for Biomedical Engineering for their friendship and emotional support during my study in Adelaide.

Finally, and most importantly, I would like to thank my parents for their support during my PhD study. If not for their kind encouragement and concern during the occasions when I was facing difficulties, I may not have been able to complete all the work presented in this thesis.

Conventions

1. **Typesetting:** This thesis is typeset using the L^AT_EX₂^ε software. TeXnicCenter 1 Beta 6.31 (Firenze) was used as an interface to L^AT_EX. Processed plots and images were generated using Matlab 7.0 (Mathworks Inc.). Adobe Illustrator (Adobe Systems Incorporated) was used to produce schematic diagrams and other drawings. Medflovon medical image processing software was developed using C++ programming language—Borland C++ Builder Version 6.0 (Borland Software Corporation). The OpenGL library (Silicon Graphics, Inc) is the application programming interface for plotting colour contour and vector flow maps.
2. **Spelling:** Australian English spelling has been adopted throughout, as defined by the Macquarie English Dictionary (A. Delbridge, Ed., Macquarie Library, North Ryde, NSW, Australia, 2001).
3. **Referencing:** Harvard style is used for referencing and citation in this thesis.

Awards

Young Investigator Award

Title: Blood flow assessment in the aortic heart valve based on magnetic resonance images using optical flow analysis

Authors: Kelvin K. L. Wong, Pawel Kuklik, Richard M. Kelso, Stephen G. Worthley, Prashanthan Sanders, Jagannath Mazumdar & Derek Abbott

Conference: XVth International Conference on Mechanics in Medicine and Biology (15th ICMMB), Singapore, 6-8th Dec 2006.

Publication: Proceedings of the XVth International Conference on Mechanics in Medicine and Biology, ISBN 1-930746-05-9, Volume 15, pages 74-76, 2006.

Outstanding Paper Award

Title: Flow imaging and validation of MR fluid motion tracking

Authors: Kelvin K. L. Wong, Richard M. Kelso, Stephen G. Worthley, Prashanthan Sanders, Jagannath Mazumdar & Derek Abbott

Conference: 13th International Conference on Biomedical Engineering (ICBME 2008), Singapore, 3-6th Dec 2008.

Publication: Proceedings of the International Federation for Medical and Biological Engineering and the 13th International Conference on Biomedical Engineering, ISBN 1680-0737, Volume 23, pages 569-573, 2008.

Publications

Journals

- WONG-K. K. L., KELSO-R. M., WORTHLEY-S. G., SANDERS-P., MAZUMDAR-J., AND ABBOTT-D. (2009). Noninvasive cardiac flow assessment using high speed magnetic resonance fluid motion tracking, *PLoS ONE*, **4**(5), Article No. e5688.
- WONG-K. K. L., KELSO-R. M., WORTHLEY-S. G., SANDERS-P., MAZUMDAR-J., AND ABBOTT-D. (2009). Medical imaging and processing methods for cardiac flow reconstruction, *Journal of Mechanics in Medicine and Biology*, **9**(1), pp. 1–20.
- WONG-K. K. L., KELSO-R. M., WORTHLEY-S. G., SANDERS-P., MAZUMDAR-J., AND ABBOTT-D. (2009). Cardiac flow analysis applied to phase contrast magnetic resonance imaging of the heart, *Annals of Biomedical Engineering*, doi: 10.1007/s10439-009-9709-y.
- WONG-K. K. L., KELSO-R. M., WORTHLEY-S. G., SANDERS-P., MAZUMDAR-J., AND ABBOTT-D. (2009). Theory and validation of magnetic resonance fluid motion estimation using intensity flow data, *PLoS ONE*, **4**(3), Article No. e4747.
- WONG-K. K. L., MAZUMDAR-J., PINCOMBE-B., WORTHLEY-S. G., SANDERS-P., AND ABBOTT-D. (2006). Theoretical modeling of micro-scale biological phenomena in human coronary arteries, *Medical & Biological Engineering & Computing*, **44**(11), pp. 971–982.
- IKBALA-M., CHAKRAVARTYA-S., WONG-K. K. L., MAZUMDAR-J., AND MANDAL-P. K. (2008). Unsteady response of non-Newtonian blood flow through a stenosed artery in magnetic field, *Journal of Computational and Applied Mathematics*, doi:10.1016/j.cam.2008.11.010.

Conferences

- WONG-K. K. L., KELSO-R. M., WORTHLEY-S. G., SANDERS-P., MAZUMDAR-J., AND ABBOTT-D. (September 2009). A novel measurement system for cardiac flow analysis applied to phase contrast magnetic resonance imaging of the heart, *Proceedings of the World Congress on Medical Physics and Biomedical Engineering*, Munich, Germany.
- WONG-K. K. L., KELSO-R. M., WORTHLEY-S. G., SANDERS-P., MAZUMDAR-J., AND ABBOTT-D. (2008). Cardiac flow characterisation based on statistical analysis of vorticity maps, *Proceedings of the SPIE Microelectronics, MEMS, and Nanotechnology (Complex Systems II)*, Melbourne, Australia, **7270**, Article No. 72700W.
- WONG-K. K. L., KELSO-R. M., WORTHLEY-S. G., SANDERS-P., MAZUMDAR-J., AND ABBOTT-D. (2008). Flow imaging and validation of MR fluid motion tracking, *Proceedings of the*

International Federation for Medical and Biological Engineering and the 13th International Conference on Biomedical Engineering (ICBME 2008), Singapore, **23**, pp. 569–573.

WONG-K. K. L., KELSO-R. M., WORTHLEY-S. G., AND ABBOTT-D. (2008). The effect of noise and sampling size on vorticity measurements in rotating fluids, *Proceedings of the International Conference on Experimental Mechanics (ICEM 2008)*, Nanjing, China.

WONG-K. K. L., KELSO-R. M., WORTHLEY-S. G., SANDERS-P., MAZUMDAR-J., AND ABBOTT-D. (2008). MR fluid motion tracking of blood flow in right atrium of patient with atrial septal defect, *Proceedings of the 5th International Conference on Information Technology and Applications in Biomedicine (ITAB 2008)*, Shenzhen, China, **1253**, Article No. 1253.

WONG-K. K. L., KELSO-R. M., WORTHLEY-S. G., SANDERS-P., MAZUMDAR-J., AND ABBOTT-D. (2007). Flow in left atrium using MR fluid motion estimation, *Proceedings of the SPIE Microelectronics, MEMS, and Nanotechnology (Complex Systems II)*, Canberra, Australia, **6802**, Article No. 68021H.

WONG-K. K. L., MOLAEI-P., KUKLIK-P., KELSO-R. M., WORTHLEY-S. G., SANDERS-P., MAZUMDAR-J., AND ABBOTT-D. (2007). Motion estimation of vortical blood flow within the right atrium in a patient with atrial septal defect, *Proceedings of the IEEE/ICME International Conference on Complex Medical Engineering (CME 2007)*, Beijing, China, pp. 862–869.

WONG-K. K. L., KUKLIK-P., KELSO-R. M., WORTHLEY-S. G., SANDERS-P., MAZUMDAR-J., AND ABBOTT-D. (2006). Blood flow assessment in a heart with septal defect based on optical flow analysis of magnetic resonance images, *Proceedings of the SPIE Biomedical Applications of Micro- and Nanoengineering III*, Adelaide, Australia, **6416**, Article No. 64160L.

WONG-K. K. L., KUKLIK-P., KELSO-R. M., WORTHLEY-S. G., SANDERS-P., MAZUMDAR-J., AND ABBOTT-D. (2006). Blood flow assessment in the aortic heart valve based on magnetic resonance images using optical flow analysis, *Proceedings of the XVth International Conference on Mechanics in Medicine and Biology (15th ICMMB)*, Singapore, **15**, pp. 74–76.

WONG-K. K. L., MAZUMDAR-J., AND ABBOTT-D. (2005). A study of the relationship between geometrical variation of atherosclerotic arteries and flow resistance, *Proceedings of the International Federation for Medical and Biological Engineering and the 12th International Conference on Biomedical Engineering (12th ICBME 2005)*, Singapore, **12**, Article No. 3A5–01.

List of Symbols

Notation	Description
B_0	Static magnetic field
B_1	Magnetic field at right angles to B_0
M_z	Net magnetisation in longitudinal alignment with B_0
μ_m	Nuclear magnetic moment in an applied magnetic field B_0
ΔE	Energy difference between the two spin states
g	Lande g-factor
\hbar	Bohr magneton constant
E	Energy of a RF photon
h	Plank's constant
ν	Frequency of a RF photon
x, y, z	Image plane coordinate system
t	Time of first exposure
δt	Exposure time delay
p	Orientation index of image set
I	Image intensity field of first exposure
J	Image intensity field of second exposure
ϵ	Higher order terms
\vec{v}	Motion of a point feature in space
∇I	Intensity spatial gradient
Ω	Interrogation spatial region
τ_D	User specified threshold
\vec{w}	Optical flow interrogation window size
\vec{d}	Intensity image displacement
L	Level number of the image pyramid
n_x	Image width
n_y	Image height
M	Number of rows
N	Number of columns

Notation	Description
$\omega(r)$	Angular velocity of vortex
$v_{\theta}(r)$	Tangential velocity of vortex
Γ	Circulation of vortex
a	Characteristic core radius
r	Radius from vortex core
θ	Angle of vortex rotation
W	Pyramidal optical flow sampling window size
W_v	Velocity inteerogation window size
E_{contour}	Energy function of active contour
E_{int}	Internal energy function of active contour
E_{ext}	External energy function of active contour
F_{int}	Internal force of active contour
F_{ext}	External force of active contour
α	Tension of active contour deformation
β	Rigidity of active contour deformation
P	Potential associated with the external forces
X, Y, Z	Image plane grid system
T	Image time grid
v^{Axial}	Two-dimensional velocity grid in axial orientation
v^{Sagittal}	Two-dimensional velocity grid in sagittal orientation
v^{Coronal}	Two-dimensional velocity grid in coronal orientation
V	Three-dimensional velocity grid system
V_R	Resultant vector magnitude
ω	Vorticity of fluid
ω_{Abs}	Magnitude value of vorticity
ω_{Dir}	Polarised value of vorticity
ω_N	Ratio of ω_{Dir} to ω_{Abs}
Φ	Shear strain rate of fluid
Ψ	Normal strain rate of fluid
μ	Mean of histogram
m	Median of histogram
$\bar{\omega}_{\mu}$	Mean of vorticity map

Notation	Description
$\bar{\omega}_m$	Median of vorticity map
$\bar{\sigma}_\mu$	Standard deviation from mean of vorticity map
$\bar{\sigma}_m$	Standard deviation from median of vorticity map
$\langle \bar{\omega}_\mu \rangle$	Temporal average of $\bar{\omega}_\mu$ values
$\langle \bar{\omega}_m \rangle$	Temporal average of $\bar{\omega}_m$ values
$\langle \bar{\sigma}_\mu \rangle$	Temporal average of $\bar{\sigma}_\mu$ values
$\langle \bar{\sigma}_m \rangle$	Temporal average of $\bar{\sigma}_m$ values
ρ	Reliability of measurement
γ	Ratio of true vorticity grid variance to a measured one
Λ_s	Vorticity grid of resolution s
Δ	Normalised error function of two vorticity grids
p_s	Pixel spacing
t_s	Trigger time interval
S	Slice thickness
p_k	Percentage of pixels in segmented flow map
A	Percentage area of region
c_j	Data cluster centroid with label j
G_j	Data cluster group based on c_j
D	Discrimination of spatial separation during data clustering
n_t	Time frame index

Abbreviations

A-P	Anterior-Posterior	36
F-H	Foot-Head	36
2C	2-chamber	32
3C	3-chamber	32
4C	4-chamber	32
SA	Short axis	32
LVOT	Left ventricular outflow tract view	32
HLA	Horizontal long axis	32
ROI	Region of interest	6, 89, 288
CW	Clockwise	162, 229
CCW	Counter-clockwise	162, 229
RA	Right atrium	32, 205
LA	Left atrium, Long axis	32, 205
RV	Right ventricle	32
LV	Left ventricle	32
AS	Anterior septum	32
IS	Inferior septum	32
SD	Septal defect	11
ASD	Atrial septal defect	204, 213
ASO	Atrial septal occlusion	204, 205, 211
FOV	Field of view	59, 60
OF	Optical flow	324
CFD	Computational fluid dynamics	8
ECG	Electrocardiogram	6, 31, 56, 148, 161
CT	Computed tomography	xi, 10, 204, 210
PET	Positron emission tomography	xi, 204
SPECT	Single photon emission computed tomography	xi, 204
NMR	Nuclear magnetic resonance	24, 26
MRI	Magnetic resonance imaging	38, 238, 255
CMRI	Cardiac magnetic resonance imaging	xi, 204
PCMRI	Phase contrast magnetic resonance imaging	3

Abbreviations

MRIV	Magnetic resonance image velocimetry	5, 13, 15
MRV	Magnetic resonance velocimetry	5
MRA	Magnetic resonance angiography	245
FID	Free induction decay	28
T1W	T_1 weighted	29
T2W	T_2 weighted	29
TE	Echo time	29
TR	Repetition time	29
PDW	Proton density weighted	29
SSFP	Steady state free precession	29, 219, 245, 284
GCFP	Global coherent free precession	245
SNR	Signal-to-noise ratio	6
RF	Radio frequency	24, 26
VENC	Velocity encoding	5, 35, 219
PIV	Particle image velocimetry	5, 15, 243, 323
API	Application Programming Interface	252
MIP	Medical image processing	251
IIL	Intel imaging library	252
IPP	Intel integrated performance primitives	252
DICOM	Digital imaging and communications in medicine	60, 190
True FISP	Fast imaging with steady-state free precession	29, 284
MEDFLOVAN	Medical flow visualisation and analysis	255

List of Figures

1.1	Overview of the thesis structure	17
<hr/>		
2.1	Quantum mechanical spin in an applied magnetic field	25
2.2	Larmor precession and resonance phenomenon	27
2.3	Profile of longitudinal and transverse magnetisation during relaxation .	28
2.4	Nature of precessing blood proton spins	31
2.5	Cardiac events with relation to the electrocardiogram	33
2.6	Cardiac magnetic resonance imaging based on different configurations .	34
2.7	Cardiac magnetic resonance image views	35
2.8	Phase contrast MRI velocimetry	35
2.9	Phase contrast MRI of a cardiac chamber	37
2.10	Velocity field of cardiac chamber	38
<hr/>		
3.1	Estimating spatial motion of pixel using optical flow	43
3.2	Multi-resolution motion estimation using pyramid implementation . . .	48
3.3	Motion estimation of in-plane MR-signals	58
3.4	Components of MR fluid motion tracking system	62
<hr/>		
4.1	Velocity characteristics of a Lamb-Oseen vortex	68
4.2	Artificial flow grid based on Lamb-Oseen vortex formulation	68
4.3	Tracking accuracy based on tangential velocities	74
4.4	Tracking accuracy based on angular velocities	78
4.5	Tracking accuracy of rotation using motion estimation algorithm	79
4.6	Tracking accuracy of rotation based on variation of noise in image	83
<hr/>		
5.1	Segmentation of atria based on active contours	92

List of Figures

5.2	A cardiac velocity visualisation system	94
5.3	Cardiac flow visualisation using streamlines	95
5.4	Three-dimensional image grid reconstruction	97
5.5	Reconstruction of flow using vectors from three orientations	98
5.6	Construction of image matrix based on five dimensions	99
5.7	Intersection nodes of a three-dimensional grid	100
5.8	Geometrical representation of plane intersection	101
5.9	Measured flow vectors in a three-dimensional space through image planes	102
<hr/>		
6.1	First order differentiation using averaging of sampled graph gradients .	109
6.2	Multi-step first order differentiation for graph with a point of inflexion .	110
6.3	Vorticity computation using finite elements	112
6.4	Shear strain computation using finite elements	113
6.5	Normal strain computation using finite elements	114
6.6	Histogram of vorticity distribution	116
6.7	Artificially generated single Lamb-Oseen vortex velocity flow field maps	121
6.8	Artificially generated double Lamb-Oseen vortices velocity flow field maps	122
6.9	Variation of grid resolution for single Lamb-Oseen vortex velocity flow field map	123
6.10	Vorticity field of Lamb-Oseen vortex (0% noise)	125
6.11	Vorticity field of Lamb-Oseen vortex (10% noise)	127
6.12	Vorticity field of Lamb-Oseen vortex (20% noise)	129
6.13	Vorticity field of double Lamb-Oseen vortices (0% noise)	131
6.14	Vorticity field of double Lamb-Oseen vortices (10% noise)	133
6.15	Vorticity field of double Lamb-Oseen vortices (20% noise)	135
6.16	Reliability test for single vortex flow fields	138
6.17	Reliability test for double vortex flow fields	139
6.18	Comparison of histograms for single vortex flow fields	141
6.19	Comparison of histograms for double vortices flow fields	142

6.20	Reliability and error deviation for multi-resolutional single vortex flow fields	143
<hr/>		
7.1	Cardiac events with relation to scan time frames	150
7.2	Cardiac vorticity visualisation system	153
7.3	MRI scan through heart for case study 1	155
7.4	MRI scan through heart for case study 2	157
7.5	Flow visualisation of normal right atrium	170
7.6	Flow quantification of normal right atrium	171
7.7	Chart of normalised vorticity mean based on a cardiac cycle	172
7.8	Qualitative visualisation of flow in the right atrium and ventricle	173
7.9	Qualitative visualisation of right atrial flow circulation	174
7.10	Flow quantification of normal left atrium and left ventricle	175
7.11	Localisation and analysis of vortices	183
7.12	Component analysis of normal right atrium flow	184
7.13	Global analysis for normal right atrium flow	185
7.14	Component analysis for normal right atrium flow	187
7.15	Variation of global vorticity mean and circulation	188
7.16	Variation of vorticity mean and circulation of vortex components	189
7.17	Magnetic resonance images of normal right atrium	191
7.18	Validation system for imaging modality based on vorticity differencing .	192
7.19	Vorticity differencing based on MR fluid motion field and phase contrast MR image field	196
7.20	Reliability of computed flow field	198
<hr/>		
8.1	Circulation in a heart with atrial septal defect	205
8.2	Schematic illustration of atrial septal occlusion	206
8.3	Myocardial discontinuity in a heart with atrial septal defect	207
8.4	Planar dissection of heart based on three MR scan slices	214
8.5	Cardiac vorticity visualisation system for ASD investigation	217

List of Figures

8.6	MRI Scans of right atrial flow pre- and post-ASO	220
8.7	Vector flow plot of right atrial flow pre- and post-ASO	222
8.8	Streamline visualisation of right atrial flow pre- and post-ASO	224
8.9	Vorticity visualisation of right atrial flow pre- and post-ASO	227
8.10	Time-variation of vorticity properties for pre- and post-ASO flow maps .	232
8.11	Summary of ASD investigation	234
<hr/>		
9.1	Stages leading to successful deliverables in the thesis	247
A.1	Three-dimensional display of MR image planes	252
A.2	Segmentation of cardiac chamber imaged by MRI	253
A.3	Velocity and vorticity flow maps superimposed onto MR image	254
A.4	Medfloan package diagram	257
A.5	Medfloan use case diagram	267
A.6	TMRI_Table class	269
A.7	TMRI_Active_Contour, TMRI_Statistics and TMRI_Draw_Parts classes . .	270
A.8	TMRI_Flow class	271
<hr/>		
B.1	Flow chart for guiding investigation of cardiac abnormalities	285
<hr/>		
C.1	Flow visualisation of normal right atrium based on one cardiac cycle . .	297
C.2	Normal atrial flow visualisation using different vorticity measurements	307
<hr/>		
D.1	Slice = 1 and time frame indices $n_t = 10$ to 13 of pre-ASO scan	310
D.2	Slice = 2 and time frame indices $n_t = 10$ to 13 of pre-ASO scan	311
D.3	Slice = 3 and time frame indices $n_t = 10$ to 13 of pre-ASO scan	312
<hr/>		
E.1	Slice = 1 and time frame indices $n_t = 10$ to 13 of post-ASO scan	314
E.2	Slice = 2 and time frame indices $n_t = 10$ to 13 of post-ASO scan	315

E.3	Slice = 3 and time frame indices $n_t = 10$ to 13 of post-ASO scan	316
<hr/>		
F.1	Thumbnails of supplementary videos	319
<hr/>		
G.1	Double vortices flow field using particle image velocimetry	327
G.2	Double vortices flow field computed by optical flow	328
G.3	Single vortex flow field computed by optical flow	329

List of Tables

3.1	MRI DICOM information used for calibration of MR fluid motion	61
4.1	Configuration characteristic of gray-scale track grid	70
7.1	Configuration of phase contrast magnetic resonance imaging	158
7.2	Configuration of phase contrast MRI and MR fluid motion tracking . . .	193
8.1	MR imaging and fluid motion tracking properties of ASD case subject .	215
G.1	PIV measurement of double vortices particle images	325
G.2	Multi-resolution OF measurement of double vortices particle images . .	325
G.3	Multi-resolution OF measurement of single vortex particle images	326